Supporting Information for

Saturation Mechanisms in Common LED Phosphors

Marie Anne van de Haar[*,1], *Mohamed Tachikirt*[1], *Anne C. Berends*[1], *Michael R. Krames*[1,3], *Andries Meijerink*[2], *Freddy T. Rabouw*[*,2]

[1] *Seaborough Research BV, Matrix VII Innovation Center, Science Park 106, 1098 XG Amsterdam, The Netherlands,*
[2] *Debye Institute for Nanomaterials Science, Utrecht University, Princetonplein 1, 3584 CC Utrecht, The Netherlands*
[3] *Arkesso LLC, 2625 Middlefield Rd, No 687, CA 94306, Palo Alto, California, USA.*

[*] Corresponding authors. E-mail: m.vandehaar@seaborough.com; f.t.rabouw@uu.nl

(5 pages including 4 figures)

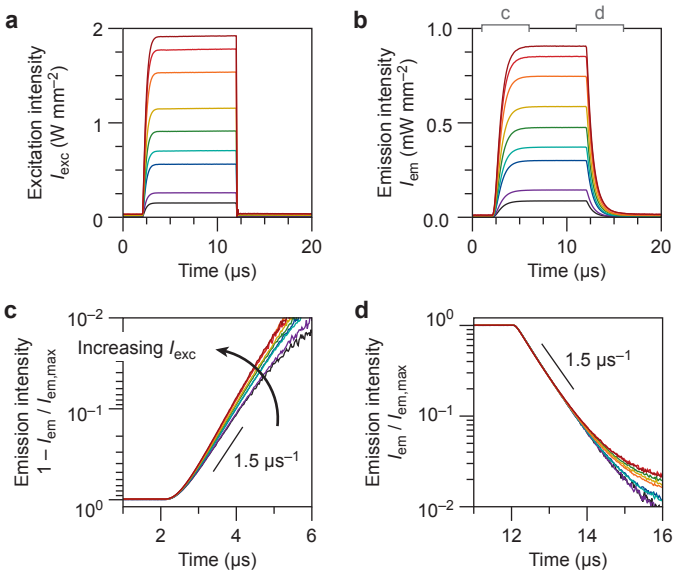

Figure S1 | Emission dynamics of CASN:Eu^{2+} under square-wave modulated excitation. **(a)** The square-wave modulated excitation intensity for different peak intensities of I_{exc} = 0.1 (black), 0.3 (purple), 0.6 (blue), 0.7 (cyan), 0.9 (green), 1.2 (yellow), 1.5 (orange), 1.8 (red), and 1.9 (dark red) W mm^{-2}. The full modulation period is 10 ms with a duty cycle of 0.1%. **(b)** The resulting emission intensity from a film of microcrystalline CASN:Eu^{2+} phosphor. **(c)** Zoom-in of the normalized rise dynamics. **(d)** Zoom-in of the normalized decay dynamics.

Figure S2 | Emission dynamics and saturation of YAG:Ce^{3+} under square-wave modulated excitation. **(a)** The square-wave modulated excitation intensity for different peak intensities of $I_{exc} = 0.3$ (black), 0.6 (purple), 1.3 (blue), 1.6 (cyan), 2.1 (green), 2.6 (yellow), 3.4 (orange), 4.0 (red), and 4.3 (dark red) W mm^{-2}. The full modulation period is 10 ms with a duty cycle of 99.8%. **(b)** The resulting emission intensity from a film of microcrystalline YAG:Ce^{3+} phosphor. **(c)** Zoom-in of the normalized rise dynamics. The dashed line shows the rise of the excitation laser (= zoom-in of the data in panel **a**). We see that the rise dynamics are determined by the slow turn-on response of the excitation laser rather than the photo-dynamics of the phosphor. **(d)** Zoom-in of the normalized decay dynamics. The dashed line shows the decay of the excitation laser (= zoom-in of the data in panel **a**). We see that the turn-off response of the excitation laser is faster than the decay dynamics of the phosphor by a factor ~ 3. **(e)** The saturation characteristics of YAG:Ce^{3+}: peak emission intensity as a function of peak excitation intensity in the square-wave experiments (both at $t \approx 0$ in panels **a,b**). The straight line is linear fit through the first four data points. Saturation sets in at $I_{exc} > 5$ W mm^{-2}. **(f)** The decay rate extracted from the data in panel **d**. All decays are slower than the reference measurement with ns-pulsed excitation presented in Fig. 1d in the main text (solid line). We conclude the slow response of the excitation laser, and possibly reabsorption of emitted light, obscure the observation of the actual decay dynamics of the Ce^{3+} centers in the phosphor. Nevertheless, the decay dynamics appear to accelerate if $I_{exc} > 5$ W mm^{-2}.

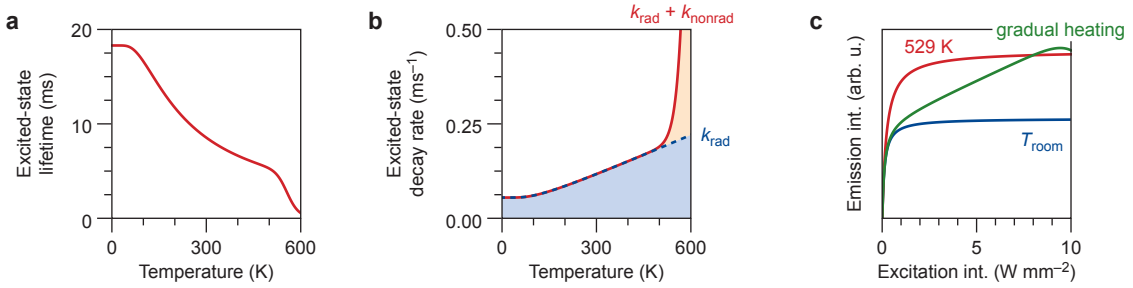

Figure S3 | Temperature-dependent decay of the Mn^{4+} ^2E excited state. **(a)** The lifetime and **(b)** the decay rate of the Mn^{4+} ^2E excited state as a function of temperature, according to Ref. S1. Radiative decay is due to phonon-assisted emission, with temperature-dependent rate

$$k_{\mathrm{rad}}(T) = k_{\mathrm{rad},0} \coth\left(\frac{\hbar\Omega}{2k_{\mathrm{B}}T}\right),$$

where $k_{\mathrm{rad},0} = 0.0546\ \mathrm{ms}^{-1}$ is the radiative decay rate at $T = 0$ K, $\hbar\Omega = 211\ \mathrm{cm}^{-1}$ is the effective energy of the phonons involved, and k_{B} is Boltzmann's constant. Nonradiative decay is due to cross-over via the $^4T_2$ state, with rate

$$k_{\mathrm{nonrad}}(T) = k_{\mathrm{nonrad},0}\, \mathrm{e}^{-\Delta E/k_{\mathrm{B}}T},$$

where $k_{\mathrm{nonrad},0}$ is the nonradiative decay rate at infinite T and ΔE is the energy barrier for cross-over. The excited-state lifetime is the inverse of the total decay rate:

$$\tau = k_{\mathrm{tot}}^{-1} = (k_{\mathrm{rad}} + k_{\mathrm{nonrad}})^{-1}.$$

(c) To model saturation with temperature-dependent radiative and nonradiative decay rates, we use that the emission intensity is proportional to the steady-state excited-state population and the radiative decay rate:

$$I_{\mathrm{em,ss}} \propto k_{\mathrm{rad}}(T)\, \frac{\sigma_{\mathrm{eff}} I_{\mathrm{exc}}/\hbar\omega}{\sigma_{\mathrm{eff}} I_{\mathrm{exc}}/\hbar\omega + k_{\mathrm{rad}}(T) + k_{\mathrm{nonrad}}(T)}.$$

The blue line shows the saturation curve for KSF:Mn^{4+} assuming a constant temperature of $T_{\mathrm{room}} = 298$ K, the red line assumes a constant temperature of $T = 529$ K. The green line is the result of a fit to the experimental data, assuming that the temperature scales with I_{exc} as

$$T = T_{\mathrm{room}} + cI_{\mathrm{exc}},$$

where c is a fit parameter, for which we find $c = 29\ \mathrm{K\,W^{-1}mm^2}$ as the optimal value. For these plots we used $\sigma_{\mathrm{eff}} = 7 \times 10^{-19} cm^2$, as determined in Fig. 4 of the main text.

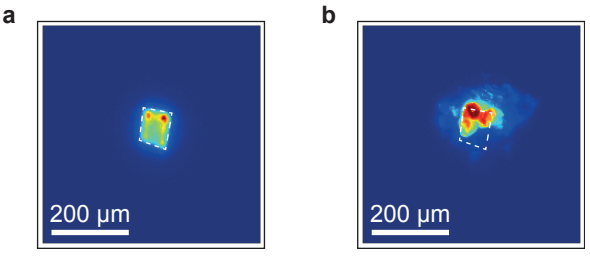

Figure S4 | Profile of the excitation spot. **(a)** Image of the luminescence from a film of microcrystalline YAG:Ce^{3+} phosphor at low excitation intensity, showing the $90 \times 90\ \mu m^2$ excitation spot with approximate square shape and only minor signal from outside the square. **(b)** Image of the luminescence from a KSF:Mn^{4+} phosphor grain extracted from the Nubia X telephone. The dashed line indicates the square-shaped excitation spot. The luminescence comes a larger area, which we ascribe to scattering by the grain.

Section S1: derivation of the rise and decay dynamics

The rate equation

$$\frac{\mathrm{d}p}{\mathrm{d}t} = k_{\mathrm{exc}}\left[1 - p(t)\right] - k_{\mathrm{decay}}p(t)$$

describes a the population evolution $p(t)$ of the excited-state of a two-level system, where k_{exc} is the rate constant for excitation and k_{decay} the rate constant for decay. This is a differential equation of the type

$$\frac{\mathrm{d}p}{\mathrm{d}t} = A + Bp(t),$$

with $A = k_{\mathrm{exc}}$ and $B = -k_{\mathrm{exc}} - k_{\mathrm{decay}}$. The general solution of this type of differential is

$$p(t) = C\mathrm{e}^{Bt} - \frac{A}{B},$$

where C is an integration constant, whose value depends on boundary conditions. We consider two situations: (1) turning on excitation at moment $t = t_1$, following a long dark period; (2) turning off excitation at moment $t = t_2$, following a long bright period.

Scenario (1) is described by the boundary condition where $p(t_1) = 0$, which sets $C = A\mathrm{e}^{-Bt}/B$. Filling this boundary condition into the general solution of the differential equation and expressing A, B in terms of the rate constant produces

$$p(t) = \frac{k_{\mathrm{exc}}}{k_{\mathrm{exc}} + k_{\mathrm{decay}}}\left[1 - \mathrm{e}^{-(k_{\mathrm{exc}}+k_{\mathrm{decay}})(t-t_1)}\right]$$

for scenario (1). This is eq 3 of the main text, where we have made the substitution $k_{\mathrm{exc}}/(k_{\mathrm{exc}} + k_{\mathrm{decay}}) = p(t_2)$ for the steady-state excited-state population that will be reached at $t \gg t_1$. We see here that the rate constant for rise, $k_{\mathrm{rise}} = k_{\mathrm{exc}} + k_{\mathrm{decay}}$, follows mathematically from the rate equation for the two-level system plus the appropriate boundary conditions.

Scenario (2) has $k_{\mathrm{exc}} = 0$, so $A = 0$ and $B = -k_{\mathrm{decay}}$. Furthermore, the boundary condition $p(t_2) = p(t_2)$ leads to $C = p(t_2)\mathrm{e}^{-Bt_2}$. Filling this into the general solution of the differential equation yields

$$p(t) = p(t_2)\mathrm{e}^{-k_{\mathrm{decay}}(t-t_2)}$$

for scenario (2). This is eq 2 of the main text.

Supporting References

(S1) Beers, W.W., Smith, D., Cohen, W.E. & Srivastava, A.M. Temperature dependence (13–600 K) of Mn^{4+} lifetime in commercial $Mg_{28}Ge_{7.55}O_{32}F_{15.04}$ and K_2SiF_6 phosphors. *Opt. Mater.* **84**, 614–617 (2018).